PLOS WATER

RESEARCH ARTICLE

Solar circulator to restore dissolved oxygen in a hypoxic ice-covered lake

Kyle F. Flynn[1,2]*, Kyle A. Cutting[3], Matthew E. Jaeger[4], Jeffrey M. Warren[3], Theodore Johnson[2], Darrin Kron[5], Chace Bell[5]

1 KF2 Consulting, Helena, Montana, United States of America, **2** CDM Smith, Inc., Helena, Montana, United States of America, **3** U.S. Fish and Wildlife Service, Red Rock Lakes National Wildlife Refuge, Lima, Montana, United States of America, **4** Montana Fish, Wildlife and Parks, Dillon, Montana, United States of America, **5** Montana Department of Environmental Quality, Helena, Montana, United States of America

* kyle.f.flynn@gmail.com

OPEN ACCESS

Citation: Flynn KF, Cutting KA, Jaeger ME, Warren JM, Johnson T, Kron D, et al. (2022) Solar circulator to restore dissolved oxygen in a hypoxic ice-covered lake. PLOS Water 1(4): e0000012. https://doi.org/10.1371/journal.pwat.0000012

Editor: Sher Muhammad, ICIMOD: International Centre for Integrated Mountain Development, NEPAL

Received: August 27, 2021

Accepted: December 16, 2021

Published: April 21, 2022

Peer Review History: PLOS recognizes the benefits of transparency in the peer review process; therefore, we enable the publication of all of the content of peer review and author responses alongside final, published articles. The editorial history of this article is available here: https://doi.org/10.1371/journal.pwat.0000012

Data Availability Statement: The final dataset are available on Dryad: https://doi.org/10.5061/dryad.m37pvmd4j.

Abstract

Hypoxia is common to shallow ice-covered lakes during the winter season, and restorative actions to prevent impacts to aquatic ecosystems are desired yet untested in remote settings. The use of a solar photovoltaic circulator was investigated for reoxygenation in a shallow hypoxic lake in the northern Rocky Mountains. During the fall of 2019, a solar powered lake circulator (SolarBee SB10000LH; hereinafter circulator) was installed near the center of Upper Red Rock Lake, Montana USA (latitude 44˚ 36'N) and dissolved oxygen (DO), temperature, turbidity, and changes to ice formation were monitored until ice-out the following spring of 2020 using an array of real-time and data logging sondes. Observations indicate the circulator formed a polynya that lasted until late November, did not increase lake turbidity, and facilitated oxygen exchange through the circulator-created-polynya for at least 3 weeks after an adjacent lake became ice covered. Thereafter, operation of the solar circulator failed from accumulation of snow and ice on the solar panels such that the lake froze completely over during a period of low light in December. From that point on throughout the winter, DO subsequently declined from supersaturation to hypoxia over a 41-day period and remained that way for nearly four months until ice-out in April. Based on this outcome, additional work is required to improve the solar-powered circulator design before attempting comparable applications elsewhere as a means of reducing the severity of hypoxia in shallow-lake systems during winter.

Introduction

Dissolved oxygen (DO), or the measure of free oxygen in water, is critical to supporting life in aquatic ecosystems [1]. Poorly oxygenated conditions have been documented in shallow ice-covered boreal and temperate lakes worldwide [2–4]. Characterized by DO concentrations <2 mgO_2/L, the onset of winter hypoxia typically begins with the physical separation of lake water from the atmosphere, which eliminates transfer of DO [5]. Surface ice and snow act as a barrier that limits air-water exchange [6] thereby reducing large scale convective and wind induced circulation within the water column [7]. Opaque surface ice and/or snow can also reduce light

Funding: This worked was funded under Montana, Fish, Wildlife & Parks (FWP) research contract #33815A. KF2 Consulting provided support for this study in the form of a salary for KFF. The Federal and State Fish, Wildlife, and Water Resource departments provided support for this study in the form of salaries for KAC, MEJ, JMW, DK, and CB. CDM Smith provided support for this study in the form of a salary for TJ. The specific roles of these authors are articulated in the 'author contributions' section.

Competing interests: The authors of this paper have read the journal's policies and declare the following competing interests: KFF is a paid consultant for KF2 Consulting and CDM Smith. KAC, MEJ, JMW, DK, and CB are paid employees of the Federal and State Fish, Wildlife, and Water Resource departments. TJ is a paid employee of CDM Smith. This does not alter our adherence to PLOS ONE policies on sharing data and materials.

penetration and photosynthetic production of oxygen by macrophytes and algae [8]. At the same time, bacterial respiration, and decomposition of organic material in the bottom sediments and suspended sediment particles in the water column continue to consume DO [9]. If the duration of ice cover lasts several months, oxygen levels continue to decrease until either hypoxia or anoxia is reached [10]. The period of low oxygen oftentimes lasts until near the break-up of lake ice during the spring [10], when oxygen exchange can resume with the atmosphere.

Lake depth is a major factor that determines if a lake becomes hypoxic during winter. In contrast to deep lakes, shallow lakes commonly undergo winter hypoxia, are commonly eutrophic, have high hydraulic residence times [11], exhibit high surface area to lake volume ratios [12], and suffer from high winter oxygen depletion rates [10, 12–14]. Additionally, the duration and spatial extent of hypoxia depends on the oxygen storage capacity of the lake prior to ice formation, and duration of ice cover [10, 14]. Factors that increase the probability of hypoxia include indirect effects of air temperature on the duration of ice-cover, snow accumulation changes on light penetration and associated photosynthetic activity by macrophytes and algae [3, 15, 16], percentage of lake volume converted to ice [17], and limited inflow or outflow exchange of water [17].

Hypoxia during winter can result in large die-offs of aquatic organisms including fish that affects species abundance, persistence, and composition [2, 17–22]. Winter is therefore considered a limiting time for many aquatic organisms in lake systems [23, 24]. Shallow lake systems with prolonged ice cover are particularly vulnerable to winterkill [25]. Decomposition and microbial processes in the benthic layer can cause long-term changes in composition of macrobenthos [26], trigger the release of potent greenhouse gases (e.g., methane and nitrous oxide; [27, 28]) or toxic levels of arsenic [29], and/or can cause changes to nutrient dynamic processes (e.g., internal regeneration or changes to nutrient cycling processes [30, 31]). Deleterious effects of winter hypoxia are therefore widespread and well-characterized, making the analysis of winterkill conditions and associated environmental management of such ecosystems a topic of high societal and conservation interest.

Many strategies have been considered to remediate hypoxia and avert large-scale winterkill of aquatic organisms [9, 10, 32–34]. Proposed restoration activities that can reverse the negative impacts of hypoxia within a winter include artificial aeration to add dissolved oxygen, snow clearing to promote in-lake photosynthesis, lake level adjustment or depth augmentation, macrophyte control which limits decomposition, and circulation enhancement (Table 1). Nearly all these approaches attempt to delay the winter oxygen depletion rate (hereafter; *WODR*) or enhance oxygen exchange with the atmosphere during the ice-on period [35].

Table 1. Literature methods used to improve winter oxygen conditions in winterkill prone lakes.

Technology Type	Methods
Artificial aeration	Compressed air injection (bubblers); mechanical surface splashers/sprayers; pump-and-baffle (cascade) aeration
Physical treatments	Snow removal; carbon application; snow fencing; submerged aquatic vegetation treatments; ground source heat pumping; molecular O_2 addition; ice removal/cutting holes in ice; pumping water onto the ice; fish population manipulation
Lake level adjustment	Dredging; dam construction; increase flow
Circulation enhancement	Inflow augmentation; pumped destratification

Source(s): [32–34, 39–41].

https://doi.org/10.1371/journal.pwat.0000012.t001

Several restorative methods tend to create an area of open water, defined as a 'polynya', to maintain oxygen exchange during the winter months between the atmosphere and water column. Oxygen transfer through the polynya occurs through surface turbulence, convective flow, and/or the displacement of warmer hypolimnetic water which creates upwelling [36, 37]. Artificial aeration has been the most widely used restorative action [33], which typically involves injection of air under the ice, aeration of a pumped water stream, surface splashers, or molecular oxygen addition [37–40]. Such efforts provide guidance for conventional artificial aeration applications to hypoxic water bodies during winter.

A crucial decision in selecting an aeration approach for ecological restoration is whether electrical power can be supplied to the site [42]. Remote geographic locations may not have access to the electrical power grid which limits the type of mechanical aeration as a means of reducing hypoxia. Ashley [40] describe pros and cons of off-grid power sources used in British Columbia for artificial aeration including: (1) generators, (2) wind power, and (3) photovoltaic (PV) systems (i.e., solar). In review, internal combustion-powered equipment (e.g., compressors or generators) are not appropriate for unattended operation in remote locations due to excessive noise pollution, emissions, refueling, and maintenance [42, 43]. Similarly, windmill aerators, while proven effective in small lakes [33, 44], require considerable up-front cost, a consistent wind source, and constant maintenance to avoid mechanical breakdowns of wind powered compressors or moving parts [33]. As a result, solar-powered circulation systems have been considered due to technological advancements in solar panels and battery storage [40, 45–47].

The use of solar-powered circulation to reduce hypoxia in lake-systems is particularly attractive due to relatively low initial costs, minimal operation and maintenance cost, low mechanical complexity, and limited carbon footprint. Ward et al. [45] document a solar circulator application in Menzies Lake, BC using a 375-watt solar panel and battery storage. That application opened a polynya 6 m across after 10 days of operation at a time when there was 0.6 m of ice depth. In a separate trial, a direct drive PV pump mounted on a raft and tested in Kilpoola Lake, BC ran for seven months through the winter without maintenance [47]. No other studies on solar-powered circulators in ice-covered lakes, or its effectiveness on promoting oxygen exchange, exist in the literature. The purpose of the current study is to document the application of a solar-powered circulator in a remote shallow lake during the winter season as a means of minimizing the duration and spatial extent of hypoxia within a lake system that routinely turns hypoxic for several months during winter. We test the hypothesis that the solar-powered circulator will lead to the formation and maintenance of a polynya, enhance DO exchange near the circulator, and result in a shorter ice-covered period, ultimately reducing the duration of under-ice hypoxia. The current study characterizes for the first time the utility of solar-powered circulation on the spatial and temporal patterns of DO during the winter season in a shallow ice-covered lake system located in a high-elevation and remote landscape.

Materials and methods

Study area

Our study focused on Upper Red Rock Lake (URRL), Montana USA (Fig 1), which is a shallow, high-elevation lake dominated by macrophytes with high potential for winterkill [48]. URRL is in a shallow postglacial wetland depression located at Red Rock Lakes National Wildlife Refuge on the western side of the Greater Yellowstone Ecosystem (GYE) [49]. URRL contains endemic Montana Arctic Grayling (*Thymallus arcticus*), which a glacial-relict population believed to be one of the few remaining viable native adfluvial (lake-dwelling) grayling

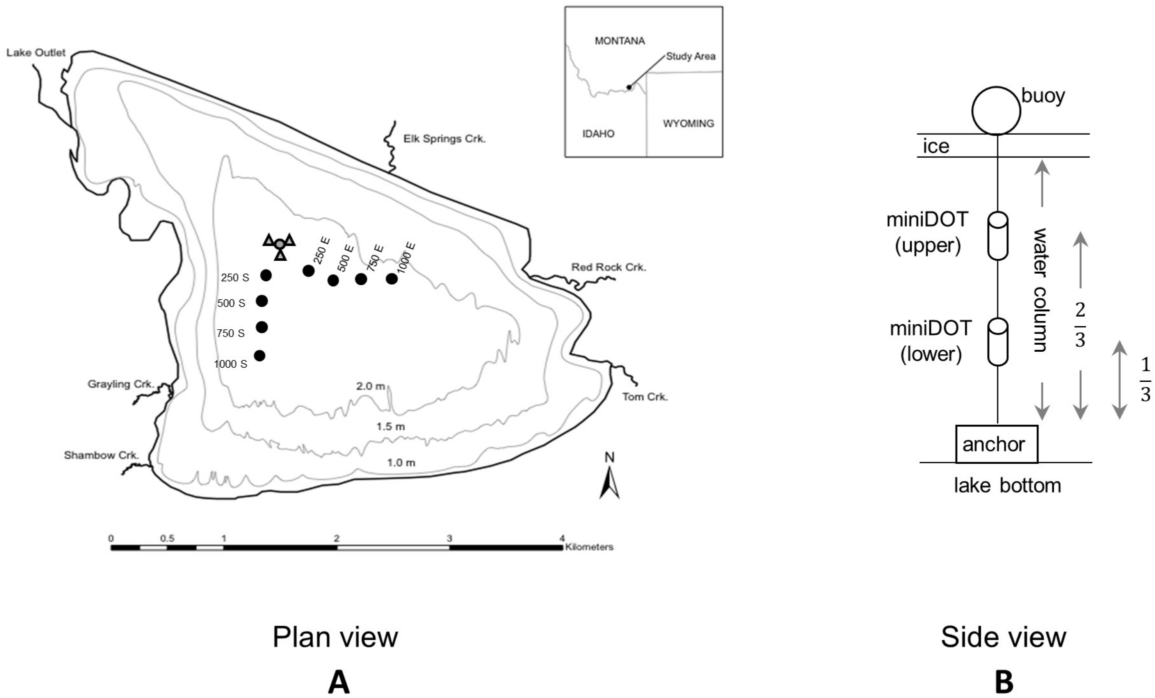

Fig 1. Upper Red Rock Lake. (a) Lake bathymetry and monitoring array configuration (solid gray circle with triangles represent location of solar circulator and real time data sonde, while solid black dots show locations of data sondes; bathymetry redrawn from Davis et al. 2019 with data from Esri Data & Maps. USA State Boundaries. 2021. Available online: https://www.arcgis.com/home/item.html?id=540003aa59b047d7a1f465f7b1df1950 (accessed on 15 May 2021). (b) Vertical configuration of MiniDOT oxygen loggers under the ice.

https://doi.org/10.1371/journal.pwat.0000012.g001

populations south of Canada and Alaska [50, 51]. The population is genetically distinct from other Montana grayling, has undergone significant range contractions, and has recently experienced a decline in both abundance and distribution [51, 52]. Given their adfluvial life history, the population resides in URRL for much of the year, except in the spring when they ascend stream tributaries to spawn [48, 53]. Prior investigators [48, 50, 53] have documented ice-covered hypoxic and anoxic conditions in URRL, noting wintertime lake conditions are believed to limit the spawning population the subsequent spring [52]. Spawning migration in grayling is largely controlled by water temperature [54]. In this regard, the cooling of water from the polynya could possibly delay migration to spawning areas.

URRL is a high elevation (2,080 m) lake with a surface area of 893 ha, maximum depth of 2 m during the ice-free season, and total water volume of 0.0128 km^3 [50, 55]. Like many high-latitude high-elevation lakes, URRL experiences long winters with ice-cover extending from November to April [50, 53]. Shallow water depths, appreciable snow and ice cover, enriched organic sediments, and abundant rooted macrophytes (*Potamogeton* spp.) contribute to declining DO levels leading to hypoxia during winter. Based on lake morphology (Table 2), winter hydraulic residence time (calculated at 143 days) is estimated to be approximately the same as the duration of ice-cover (165 days), with a sediment surface area to lake volume ratio of 0.93, signifying extremely high *WODR* [12] (S1 Table). Due to appreciable winds and lack of stratification, URRL is believed to be polymictic and should be fully aerated at the time of ice cover. URRL is a designated wetland Wilderness area and is part of the largest wetland complex in the GYE [56]. Permission was obtained from Red Rock Lakes National Wildlife

Table 2. Morphometric and environmental characteristics of Upper Red Rock Lake, Montana, USA.

Attribute	Quantity	Source
Surface Area	893 ha	[49]
Volume	0.0128 km^3	[49]
Depth (mean | max)	1.4 m | 2 m	[49]
Inflows (winter conditions)		
Red Rock Creek	0.572 m^3/s	[57]
Tom Creek	0.047 m^3/s	
Elk Springs Creek	0.278 m^3/s	
Shambow Creek	0.058 m^3/s	
Grayling Creek	0.079 m^3/s	
Hydraulic Residence Time	143	[57]
Elevation	2,080 m AMSL	[47]

https://doi.org/10.1371/journal.pwat.0000012.t002

Refuge to access the study site and a scientific collector permit was not required for this study since only abiotic parameters were measured and all installed instrumentation was temporary.

Solar circulator

On 26 September, 2019, a SolarBee SB10000LH [58] PV lake circulator (Fig 2) was installed near the west-central portion of URRL for operation during the winter season. The SolarBee is an updraft, low head, high volume axial pump, designed to circulate large volumes of water (up to 0.631 m^3/s) upward through a draft tube and then laterally, distributing oxygenated water outward using an impeller and distributor dish. A single SolarBee is reported to be able aerate a small ice-free 10-ha area [58] and is powered by three mono-crystalline 90 watt (W) photovoltaic modules totaling 270 W that do not require direct sunlight with battery storage for up to 24-hour operation during low light conditions [59, 60]. Electronic logs attached to a SB10000LH unit indicate they run continuously throughout the year at 98% full speed in northern latitudes (personal communication, J. Bleth Medora Corporation, April 9, 2019). During periods of prolonged inclement weather, oiled freeze sleeves on the impeller shaft

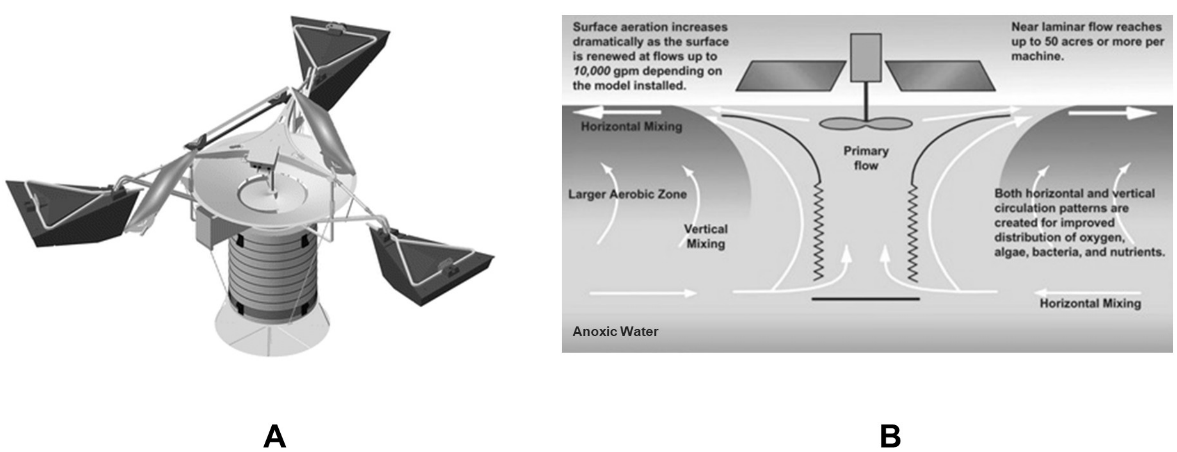

Fig 2. SolarBee circulator [58]. (a) 3D drawing of the floats and draft tube. (b) Diagram illustrating how the SolarBee mixer circulates large volumes of water upward through a draft tube then laterally distributing oxygenated water using an impeller and distributor dish (figure modified from manufacture website).

https://doi.org/10.1371/journal.pwat.0000012.g002

allow the shaft to turn freely inside the sleeve if ice forms over the lake or waterbody in which the unit is installed.

The SolarBee is designed for remote settings as it requires only sunlight for power generation (a renewable energy source), has no emissions, requires no ground disturbance, produces minimal sound, and generates electricity with no moving parts and little maintenance [58]. Lastly, it was ideal for shallow depth application as the machine's intake (draft tube) can be set to mix only the top 1 m of water without disturbing the bottom 1 m, which minimizes sediment resuspension, especially critical for our study site. Finally, no published studies document SolarBee application under severe winter conditions.

Lake monitoring

To assess the duration and effectiveness of the PV circulator's influence on winter conditions, DO, water temperature, and turbidity measurements were made continuously in the vicinity of the circulator. A NexSens CB-50 data buoy with an iridium satellite telemetry option, equipped with YSI EXO2 datasonde was tethered to one of the floats on the circulator (latitude 44˚ 36' 43.488" N, longitude 111˚ 43' 41.412" W). The sonde was positioned at a depth of 0.89 m (total depth of water column is 1.59 m so it was located at 56% of the total depth) and measured the following attributes at two-hour intervals beginning on 25 October, 2019: temperature (˚C), dissolved oxygen (mg/L and % saturation), pH (S.U.), specific conductivity (μS/cm), and turbidity (NTU). Real-time observations from the sonde were uploaded via satellite transmission using WQData LIVE. To measure the spatial extent of the affected area caused by the solar circulator, two transects of Precision Measurement Engineering miniDOT dataloggers were installed once the ice was safe enough to walk on 19 December, 2019. Holes were augured in the ice with a hand auger (10 cm diameter). Dataloggers were spaced radially from the PV circulator at the following distances in the south and east directions (Fig 1a and S2 Table): (1) 250 m, (2) 500 m, (3) 750 m, and (4) 1000 m based on observed gradients and oxygen isopleths from [37]. Loggers were vertically deployed at 1/3 and 2/3 the overall depth of the water column (Fig 1b, S2 Table). Individual miniDOT loggers were set to log at an interval of every 10 minutes with an accuracy of ±0.3 mg L^{-1} and ±0.10˚C [61]. Air temperature data was obtained from a nearby weather station, Red Rock RAWS RRDM8 near Lakeview (latitude 44˚ 40' 59" N, longitude 111˚ 49' 59" W), located 12 km northwest and 22 m above the lake elevation [62].

Statistical analyses

Data were analyzed using statistical and graphical procedures in R [63], including rLakeAnalyzer [64] and gStat [65]. Inverse distance weighting (IDW) procedures for spatial data analysis employed a pixel size of 10 m. While certain authors choose to analyze time-series in both the time and frequency domain, i.e., to better understand time scales and processes responsible for response variables; [66, 67], we elected to use simplistic methods since our objective was to document solar circulator winter performance relative to the temporal and spatial patterns of DO under the ice.

Results

Surface conditions of URRL were visually observed approximately monthly and followed the seasonal progression shown in Fig 3. Beginning with ice-free conditions in October, the lake progressed into consolidated ice by 28 October, with an ~25 m diameter polynya on 7 November. Following this cold period in late-October/early-November, the polynya increased to ~65 m diameter on 25 November. The polynya remained ice-free until at least 25 November, indicating the polynya was ice-free for 30–40 days longer than the other parts of the lake. After this

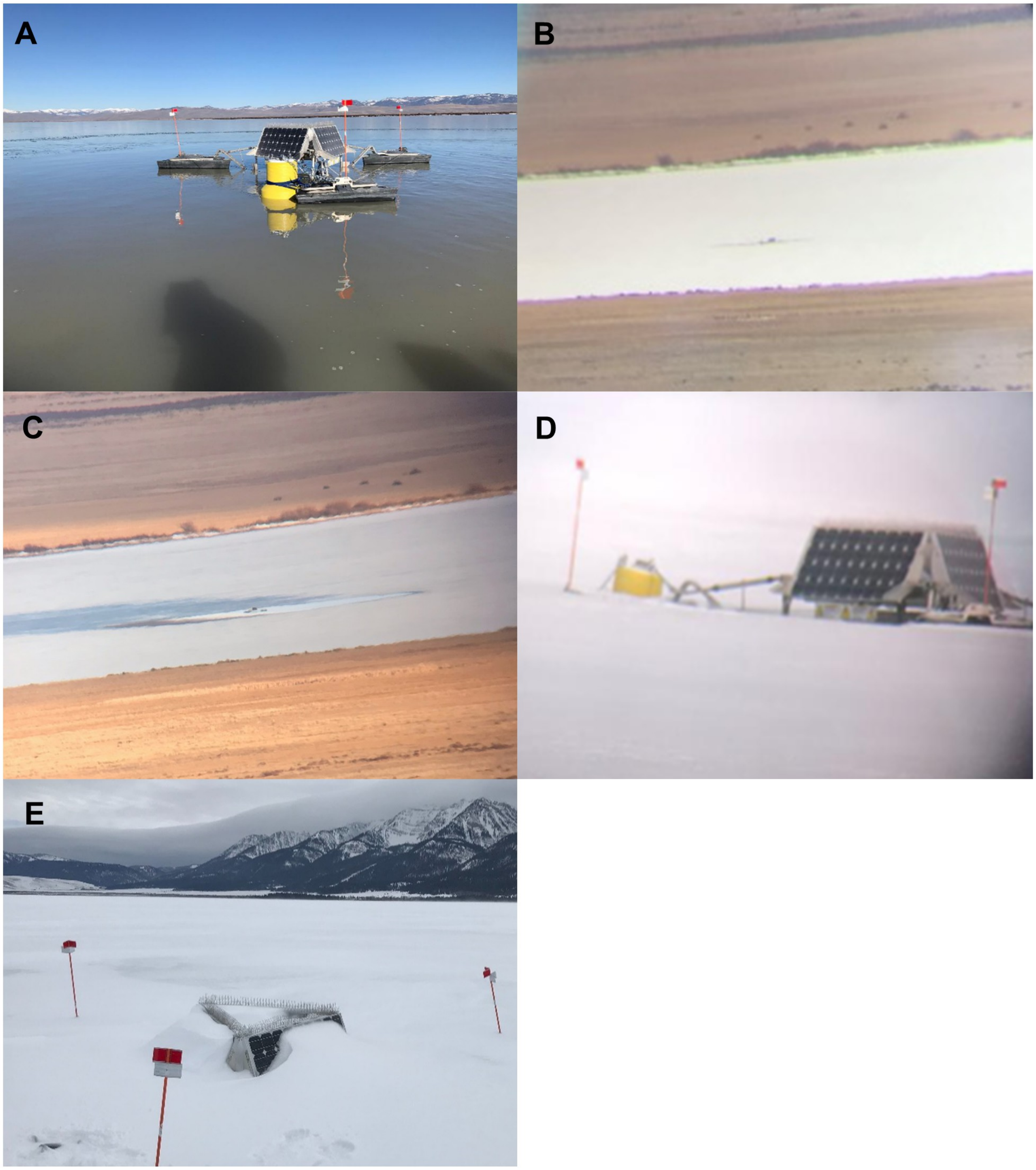

Fig 3. Photo series of SolarBee installation during the transition from fall-to-winter of 2019 to 2020. (a) 26 September, 2019 –open water deployment. (b) 7 November, 2020 –Circulator operational and ~ 25m polynya present. (c) 25 November, 2020 –Circulator operational and ~65m polynya present. (d) 19 December, 2020 –unit frozen into the ice but still operational. (e) 21, January, 2020 –Circulator is non-functional and buried in snow such that solar panels are barely visible.

https://doi.org/10.1371/journal.pwat.0000012.g003

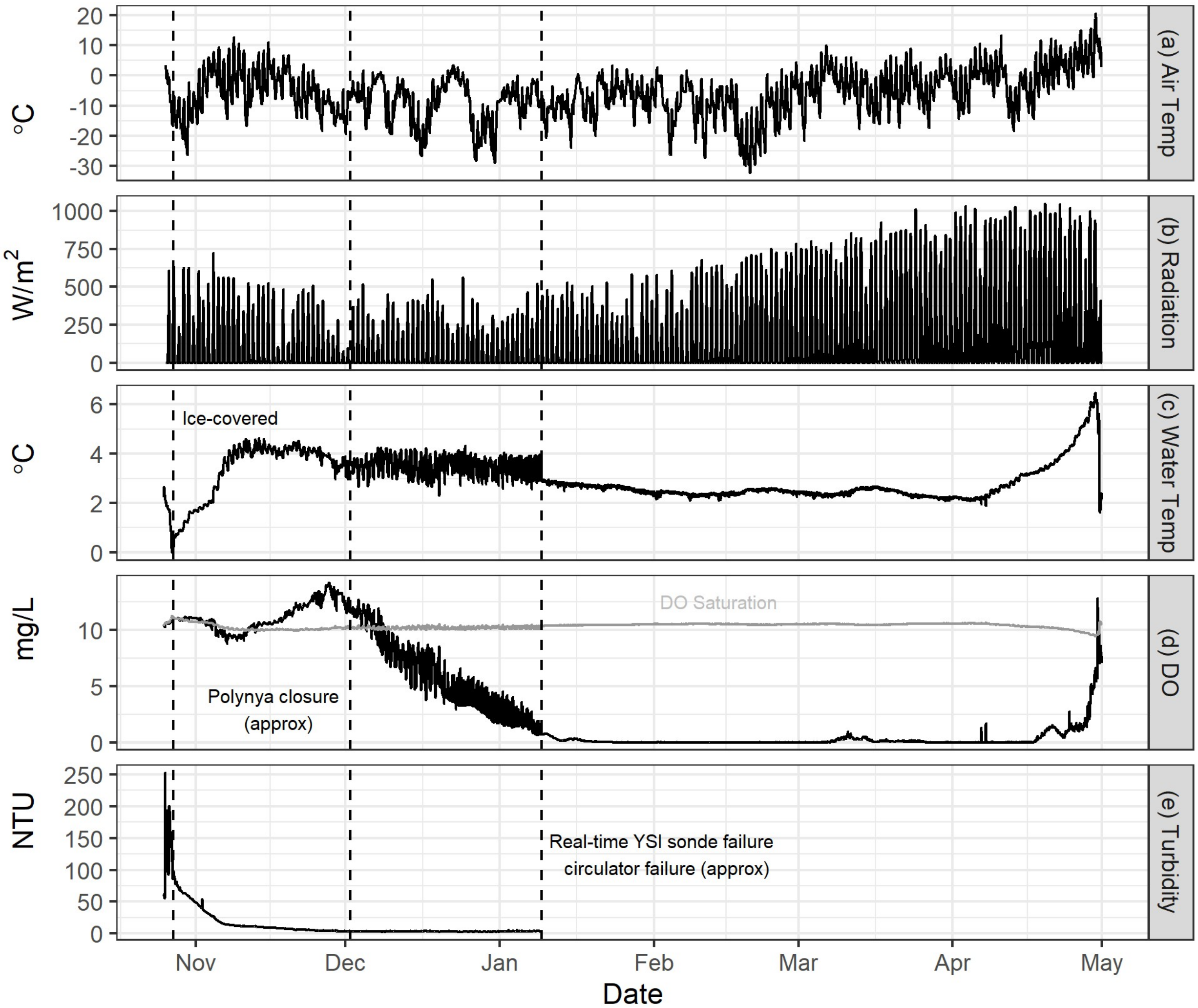

Fig 4. Meteorological, YSI EXO2 sonde, and miniDOT data recorded in URRL during the winter of 2019 through 2020. (a) Air temperature. (b) Solar radiation. (c) Water temperature. (d) Dissolved oxygen (DO) and DO saturation as calculated by elevation and water temperature, and (e) turbidity. Note: Real-time YSI sonde failure on 1/9/2020 denoted by the dashed vertical lined; data were substituted with the average of the most proximal miniDOT loggers (i.e., 250 m away).

https://doi.org/10.1371/journal.pwat.0000012.g004

date, the polynya froze, and became heavily snow-covered by 19 December. The solar circulator was still in operation on 19 December.

DO concentrations prior to ice-on (i.e., late-October), were 10.5 mgO_2/L (~100% of saturation), water temperature of 2–3˚C, with a turbidity of 250 NTU (Fig 4). Water temperature at the YSI sonde was 0˚C on 27 October, 2019 and warmed slowly thereafter to 4˚C, an indicator of ice-covered conditions whereby heat flux from the lakebed rewarms the water column [38, 68]. Air temperature during this time was generally below freezing and visual observations suggest several cycles of freezing and reopening prior to complete ice establishment.

Over the next 3 weeks, a polynya was present at the solar circulator that resulted in water/atmospheric oxygen exchange. The polynya then fully iced over sometime in late-November to early-December and the circulator eventually became non-operational sometime between December 20, 2019 and January 21, 2020 due to snow and ice cover on the solar panels. The real-time YSI datasonde buoy (also charged by solar panels) experienced a similar fate with the last communication occurring on 09 January, 2020 11:00:00, approximately three weeks after the continuous recording MiniDOT dataloggers were deployed.

DO initially increased in URRL after ice-on in late-October (Fig 4) going from saturation (10.5 mgO_2/L) to approximately 140% of saturation (>14 mgO_2/L), presumably from macrophyte photosynthesis. We then observed a nearly linear decline over a 41-day period beginning from 29 November, 2019 to 09 January, 2020 when the YSI sonde failed. During this time DO dropped from 13.5 to 1.6 mg/L, which equates to a localized *WODR* of 0.21 $gO_2/m^2/d$ (assuming a depth of 1.4 m). Lake DO level declined further thereafter, nearly reaching anoxic conditions (<0.1 mg/L) in late winter as will be discussed subsequently. At the same time background turbidity levels fell to between 3 and 5 NTU due to cessation of large-scale turbulent wind mixing in conjunction with under-ice particle settling.

MiniDOT array data provide an understanding of 2- and 3-dimensional lake processes, filling the temporal data gaps identified earlier. Two types of spatial gradients were noted in the water column. In most cases, a vertical gradient in DO was noted. Concentrations at the top of the lake were higher than the bottom during the initial ice cover (Fig 5). This was found to occur until early-February when the entire array experienced near anoxic conditions that persisted until mid-April. Unexpectedly, and in advance of ice breakup on 28 April, 2020, DO at the bottom sonde rebounded two weeks sooner and was appreciably higher than the top sonde DO suggesting a possible lakebed DO source.

The dynamic nature of the water column during the deployment period from 20 December, 2019 through 30 April, 2020 is documented for vertically nested dataloggers at 500 S (Fig 6), indicating rapid winter depletion and then reoxygenation of water in the vicinity of the circulator. It is important to note that the circulator did not turn back on during spring and miniDOT loggers observed a return to atmospheric saturation, reflecting complete mixing of the shallow system coinciding with spring ice breakup during last week of April. Prior to ice-off we note the possibility of an under-ice bloom for a brief period as DO was supersaturated, an occurrence which has been reported by others [69].

A DO gradient was also observed extending outward from the solar circulator with the highest oxygen concentrations occurring near the circulator, declining radially, and changing rapidly through time (Fig 7). In this regard, we believe the circulator did enhance DO concentrations up to 1000 m away from the unit during a short transitional period between early to late November when a polynya was present, and the lake was below oxygen saturation. The oxygenated area closed quickly thereafter. Macrophyte photosynthesis then supersaturated the water column until the ice become snow covered, the plants senesced, and DO depletion became dominant. DO and temperature levels were surprisingly different in the southern and eastern miniDOT arrays, indicating a lack of symmetry about the circulator likely due to lake currents driven by the slope of the lakebed as under-ice water flowed towards the outlet of the lake in the northwest corner. As anticipated, water temperature during ice-cover was consistently warmer near the bottom than the top due to sediment heat flux which causes inverse stratification since water is most dense at 4.0˚C (S1 Fig). Over the course of the winter, water temperature ranged from approximately 2 to 4˚C prior to ice off in the last week of April, noting changes in water temperature at the top position along the 1000-m transect largely mirrored the lower, albeit 2 to 3˚C cooler. Changes in water temperature along the 1000-m transect at the bottom were warmer (~4.0˚C) along the east than south (3 to 3.5˚C) transect. Weak inverse stratification was present near circulator as noted by difference (Δ) between the bottom and top logger, relative to adjacent loggers which were more strongly stratified (S2 Fig), suggesting the circulator was indeed influencing under-ice water movements.

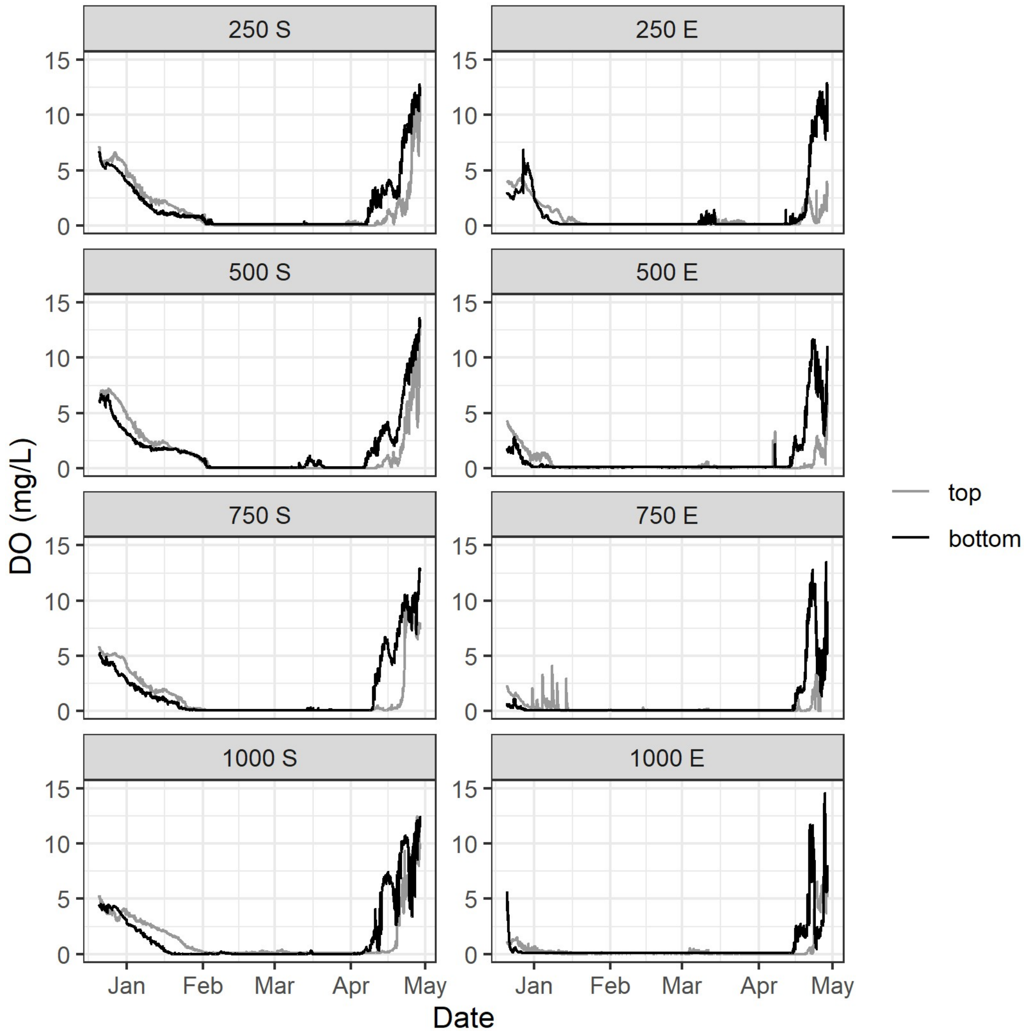

Fig 5. Dissolved oxygen data near the solar circulator recorded at the top (1/3 depth) and bottom (2/3 depth) of the water column in the monitoring array. Distances (m) away from SolarBee are denoted in titles of figure panels for the south (S) and east (E) transects (e.g., 250 S = 250 m south of the circulator). The diameter of the polynya on 25 November was 26% and 6.5% of the 250-m and 1000-m long spacing, respectively.

https://doi.org/10.1371/journal.pwat.0000012.g005

Discussion

Vertical circulation of lakes has been proposed to increase dissolved oxygen for aquatic ecosystem restoration; however, few studies have documented the efficacy of ultra-low head, large flow PV circulation during winter months in remote settings. Ashley [40]) describes this technology at preventing winterkill of aquatic organisms in northern latitudes, and Ward et al. [45] used a Wardun WD 20 Sunstirrer unit to create a 120 m^2 polynya after 10 days of trial operation during winter. The batteries in this unit however were soon depleted to between 1/3 to 1/2 full charge following a five-day snowstorm, resulting in a significant reduction in oxygen exchange across the air-water interface [47]. Results from the current study suggest the solar circulator in general, experience similar issues and may not be a feasible alternative for long-term remote unattended operation throughout the winter season. For instance, daily incoming global solar radiation on winter solstice in 2019 was 59 W/m^2, which is slightly greater than

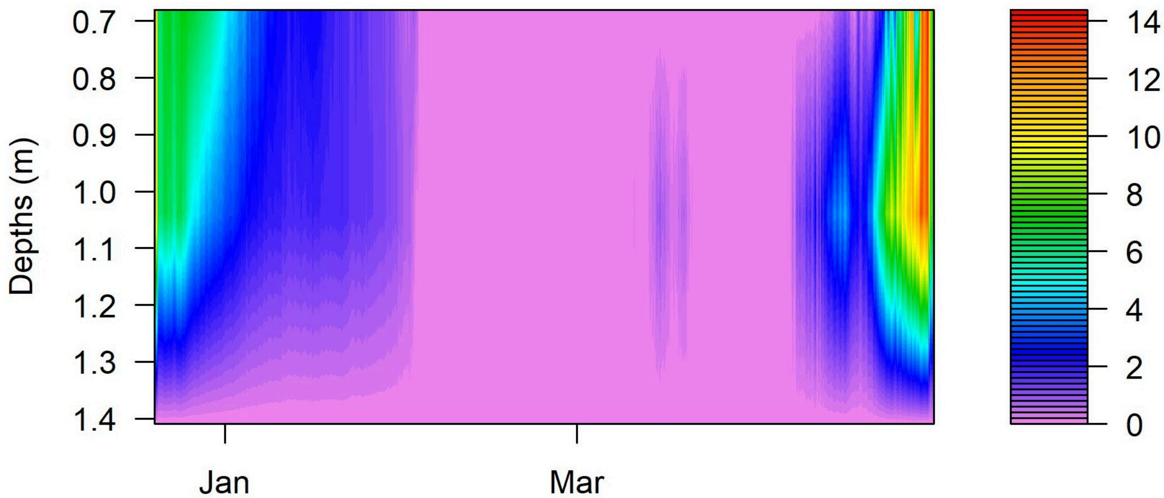

Fig 6. Temporal changes in the vertical DO gradient in the water column 500 m south of solar circulator, December 20, 2019 through April 30, 2020. Interpolation assumes DO = 0 mg/L at the lakebed.

https://doi.org/10.1371/journal.pwat.0000012.g006

the motor's operating power requirement of 40 to 50W. However, during the time of polynya closure in late-November to early-December, two- and five-day average incoming solar radiation was just 19 W/m^2 and 34 W/m^2 (Fig 4). This demonstrates the energy dilemma for winter circulation. While on clear-sky days there is enough watt-hours of energy to power the motor during the day and nighttime and charge the batteries, the influence of multi-day cloudy, inclement weather on power generation appears to be a limitation. A need exists for advanced power generation or battery storage that can extend period of operation during inclement weather, or when charging is not available (e.g., nighttime).

A supplemental generator in the form of a small wind microturbine [70], with enhanced battery storage technology (e.g., lithium-iron-phosphate battery or ultra-low temperature battery technology), could potentially extend the operation of the solar circulator during the winter months. URRL is often windy and although the wind would be insufficient on its own to solely source wind power [57], it may be an excellent companion technology to solar-based power circulation. Another issue is fouling of the solar panels. As noted in Figs 2 and 3, the SolarBee solar panels are in close vertical proximity to the water/ice surface such that coverage from wind drift of snow and ice is a problem at recharging the batteries. Future applications could consider elevated panels, or panels that have wipers to prevent accumulation of blowing or drifting snow.

A secondary consideration is whether the circulator decreased the duration of ice-cover, which can shorten the oxygen-exchange time between the water and atmosphere. During our study, the period of ice-cover lasted at approximately 183 days, extending from 27 October, 2019 to the last week of April, 2020. However, the lake did not fully freeze until at least late-November at the circulator, even though the rest of the lake, and an adjacent lake, had become iced over prior to that time. This suggests a localized decrease in ice-cover duration of approximately 30 to 40 days (i.e., ~20% of winter), and that the polynya surrounding the solar circulator created an oxygenated area in the vicinity of the circulator (Fig 6).

Many researchers refer to ice-on and ice-off as an event that occurs over a single day [71, 72]. Recent high-frequency data suggests it is a longer process taking upwards of several days to weeks [67, 72]. We confirmed multiple freeze and thaw episodes visually at URRL and note

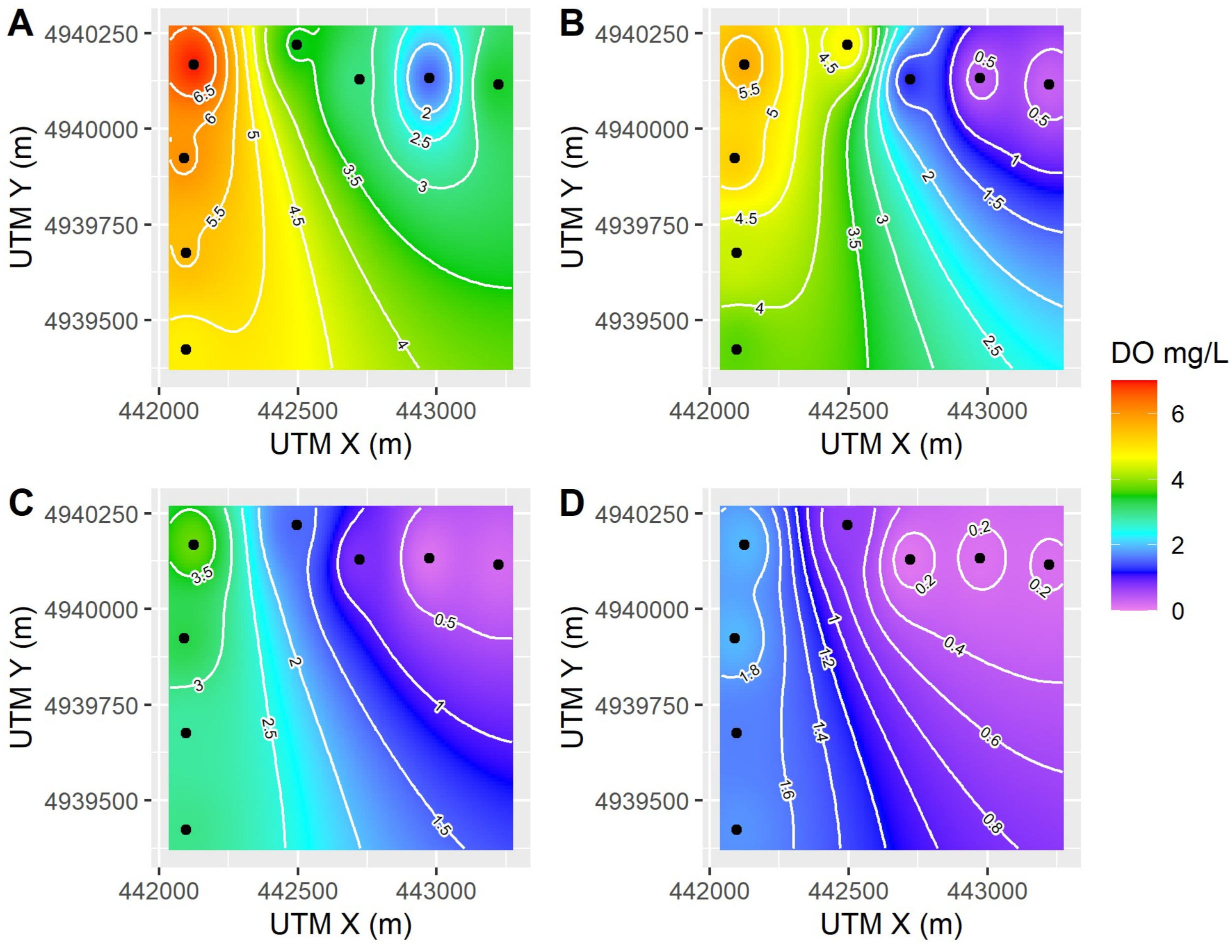

Fig 7. Horizontal DO gradients in the vicinity of the solar circulator at one-week intervals after the closure of the polynya taken as the average of the top and bottom miniDOTs at midnight. (a) December 21, 2019 (shortly after miniDOT deployment), (b) December 28, 2019, (c) January 4, 2020, and (d) January 11, 2020.

https://doi.org/10.1371/journal.pwat.0000012.g007

that quantifying a statically based decrease in the period of ice-cover is difficult. The duration of ice cover at URRL was reported to be 143 and 124 days during the winters of 2013–2014 and 2014–2015, respectively [48]. This is considerably shorter than was observed in 2019–2020 (i.e., 183 days). In this regard, the duration of ice cover surrounding the circulator, while decreased by about 4 weeks, was still longer than in previous years and probably did not meaningfully contribute to a reduction in lake ice cover or the number of days of hypoxia experienced around the circulator.

Barica and Mathias [10] and Ellis and Stefan [9] indicate that winterkill lakes behave as closed systems, such that the critical time to reach hypoxia is a function of the initial oxygen storage at the time of freezing and the winter DO depletion rate caused by sediment and/or biochemical oxygen demand. In the current study, DO in URRL was approximately 100% of atmospheric saturation at the time of freezing (Fig 4). Furthermore, the water became supersaturated from photosynthetic activity by macrophytes, which has been reported in other shallow productive systems [41]. Dynamic changes in DO brought about by under-ice biological processes add complexity to the use of solar circulators.

Another under-ice consideration is suppression of the initial oxygen storage from suspended organic particles and biochemical oxygen demand [73], which could have dramatic consequences on the ability to overwinter fish and may shorten the time to anoxia [10]. In this case, URRL turbidity was high at the time of freezing in the fall; however, macrophyte photosynthetic oxygen production sufficiently overcame the oxygen sink from suspended particles until the turbidity under the ice declined. Snow-clearing has been proposed as a potential remedy to increase macrophyte production [32]. However, a practice such as this is challenging especially in remote locations with considerable amounts of snowfall and wind drifting.

As noted in the current and previous studies [3, 5, 6], DO concentrations are heterogeneously distributed in the water column of ice-covered waterbodies and are often depth- and/or location-dependent due to water inputs (i.e., tributaries), sediment-water interactions, under-ice photosynthesis, or other waterbody-morphometric features. Even with artificial circulation in URRL, DO gradients (Figs 6 and 7) and thermostratification (S1 Fig) were noted both in vertical and horizontal directions around the circulator. The lack of horizontal symmetry was particularly surprising, and it is unclear if this was related to ice-cover variability over the entire lake, stream inflows, or some other spatial phenomenon (e.g., convective currents or under ice seiche [74, 75]) that we were unable to ascertain given the available data. Possibly the gradient could have been a transient remnant of localized DO at the circulator center that was depleted over time due to horizontal diffusion and SOD.

In closed-basin and shallow-lake systems, the highest oxygen concentrations typically occur directly under the ice and decline with depth [17, 48]. Prior investigators note in some instances fish have been shown to avoid hypoxic conditions by either moving to the ice-water interface, towards highly oxygenated stream inlets, or migrating entirely from the lake [48, 70]. As is the case of our study system, Arctic grayling select areas with deeper and more well-oxygenated waters along with congregating near stream tributaries [48, 50]. In this regard, understanding the contribution of dissolved oxygen sources reoxygenating the water column from either macrophyte or plankton photosynthesis, tributary sources, or groundwater inflow require further investigation [75].

Potential limitations and hazards of solar-circulation devices should be recognized. These include whole lake cooling from increased exposure to the atmosphere [76], resuspension of sediments due to mixing [39], increases in sediment oxygen demand rates [9, 33], and open water conditions that create a hazard to winter lake recreation or wildlife [9]. It is believed negative outcomes such as these were largely minimized in our study based on evidence that only a small polynya (~65 m in diameter) was present and for a limited duration during early winter (limiting thermal loss), turbidity during the circulation period following ice cover as turbidity was <5 NTU (sediment resuspension was not a concern), and the remote location of our study site largely precluded hazards to recreationalists or wildlife.

Finally, it is important to recognize that prior experience with solar circulator technology in shallow ice-covered lakes is limited. Solar circulators have been used in deeper lakes during winter months [45, 47], or for reservoir mixing or destratification and aeration of effluents discharged from wastewater treatment facilities during open water conditions [59]. Based on the current study, we are of the opinion that applications in shallow lakes at similar latitudes and extreme winter conditions for ecological restoration purposes will be of limited success without additional technological development. Future research into renewable lake aeration technologies should be undertaken to address the abovementioned limitations before practitioners can remedy hypoxic conditions during the winter using such technology.

Conclusion

We found the use of a solar circulator to be insufficient for maintaining an open water polynya or for appreciably improving dissolved oxygen concentrations throughout the entire winter.

We found the circulator may have improved DO conditions for upwards of 30–40 days during the initial ice cover but then failed during the subsequent winter months during times of low incident radiation. Despite the limitations of our results, solar-powered circulation methods should not be discarded but rather necessitate additional research and development. A primary benefit of solar circulators is that they only require sunlight as a power supply, there are no direct fossil fuel emissions, and they can generate electricity with no moving parts and little maintenance. However, the use of solar mixers at restoring under-ice hypoxia thereby improving conditions for aquatic organisms (e.g., fish) is limited at this time. Additional research should be pursued to better understand the benefits and limitations in hostile environments where species of high conservation concern reside.

Supporting information

S1 Table. Reported winter oxygen depletion rates.
(DOCX)

S2 Table. Location and summary of monitoring instrumentation.
(DOCX)

S1 Fig. Water temperature data near the solar circulator array.
(TIFF)

S2 Fig. Strength of stratification in the vicinity of the solar circulator at one-week intervals after the closure of the polynya taken as the difference (Δ) between the bottom and top miniDOTs at midnight. (a) December 21, 2019 (shortly after miniDOT deployment), (b) December 28, 2019, (c) January 4, 2020, and (d) January 11, 2020.
(TIFF)

Acknowledgments

We thank the staff at Red Rock Lakes National Wildlife Refuge, especially Cortez Rohr and Mike Bryant, along with Lucas Bateman and Tim Gander of Montana Fish, Wildlife & Park for field support.

Author Contributions

Conceptualization: Kyle F. Flynn, Kyle A. Cutting, Matthew E. Jaeger, Jeffrey M. Warren, Theodore Johnson.

Data curation: Darrin Kron, Chace Bell.

Formal analysis: Kyle F. Flynn, Theodore Johnson.

Funding acquisition: Matthew E. Jaeger.

Investigation: Kyle F. Flynn, Kyle A. Cutting, Matthew E. Jaeger.

Methodology: Kyle F. Flynn, Kyle A. Cutting, Matthew E. Jaeger.

Project administration: Kyle F. Flynn, Kyle A. Cutting.

Resources: Kyle A. Cutting, Matthew E. Jaeger, Darrin Kron, Chace Bell.

Software: Kyle F. Flynn.

Supervision: Kyle F. Flynn, Kyle A. Cutting.

Validation: Kyle F. Flynn, Kyle A. Cutting.

Visualization: Kyle F. Flynn, Kyle A. Cutting.

Writing – original draft: Kyle F. Flynn.

Writing – review & editing: Kyle F. Flynn, Kyle A. Cutting, Matthew E. Jaeger, Jeffrey M. Warren, Theodore Johnson, Darrin Kron, Chace Bell.

References

1. Davis JC. Minimal dissolved oxygen requirements of aquatic life with emphasis on Canadian species: A review. Journal of the Fisheries Board of Canada. 1975; 32(12): 2295–2332.
2. Greenbank J. Limnological conditions in ice-covered lakes, especially as related to the winter-kill of fish. Ecol Monogr. 1945; 15: 343–392.
3. Kirillin G, Leppäranta M, Terzhevik A, Granin N, Bernhardt J, Engelhardt C, et al. Physics of seasonally ice-covered lakes: a review. Aquatic Sciences. 2012; 74: p. 659–682.
4. Yang B, Young J, Brown L, Wells M. High-frequency observations of temperature and dissolved oxygen reveal under-ice convection in a large lake. Geophysical Research Letters. 2017; 44(24).
5. Wetzel RG. Limnology. 2nd ed. Philadelphia: Saunders College Publishing; 1983.
6. Golosov S, Maher OA, Schipunova E, Terzhevik A, Zdorovennova G, Kirillin G. Physical background of the development of oxygen depletion in ice-covered lakes. Oecologia. 2007; 151: 331–340. https://doi.org/10.1007/s00442-006-0543-8 PMID: 17115190
7. Malm J, Bengtsson L, Terzhevik A, Boyarinov P, Glinsky A, Palshin N, et al. Field study on currents in a shallow, ice-covered lake. Limnol Oceanogr. 1998; 43(7): 1669–1679.
8. Welch HE, Kalff J. Benthic photosynthesis and respiration in Char Lake. Journal of the Fisheries Research Board of Canada. 1974; 31(5): 609–620.
9. Ellis CR, Stefan HG. Oxygen demand in ice covered lakes as it pertains to winter aeration. Water Resources Bulletin. 1989; 25(6): 1169–1176.
10. Barica J, Mathias JA. Oxygen depletion and winterkill risk in small prairie lakes under extended ice cover. Journal of the Fisheries Research Board of Canada. 1979; 36(8): 980–986.
11. Nürnberg GK. Quantification of oxygen depletion in lakes and reservoirs with the hypoxic factor. Lake Reserv Manag. 2002; 18(4): 299–306.
12. Mathias JA, Barica J. Factors controlling oxygen depletion in ice-covered lakes. Can J Fish Aquat Sci. 1980; 37(2): 185–194.
13. Babin J, Prepas EE. Modeling winter oxygen depletion rates in ice-covered temperate zone lakes in Can J Fish Aquat Sci. 1985; 42(2): 239–249.
14. Terzhevik A, Golosov S, Palshin N, Mitrokhov A, Zdorovennov R, Zdorovennova G, et al. Some features of the thermal and dissolved oxygen structure in boreal, shallow ice-covered Lake Vendyurskoe, Russia. Aquat Ecol. 2009; 43: 617–627.
15. Wright R. Dynamics of a phytoplankton community in an ice-covered lake. Limnol Oceanogr. 1964; 9 (2): 163–178.
16. Baehr MW, Degrandpre MD. Under-ice CO2 and O2 variability in a freshwater lake. Biogeochemistry. 2002; 61(1): 95–113.
17. Cott PA, Sibley PK, Somers WM, Lilly MR, Gordon AM. A review of water level fluctuations on aquatic biota with an emphasis on fishes in ice-covered lakes. J Am Water Resour Assoc. 2008; 44(2): 343–359.
18. Cooper GP, Washburn GN. Relation of dissolved oxygen to winter mortality of fish in Michigan Lakes. Trans Am Fish Soc. 1949; 76(1): 22–33.
19. Hughes GM. Respiratory responses to hypoxia in fish. Am Zool. 1973; 13(2): 475–489.
20. Danylchuk AJ, Tonn WM. Natural disturbances and fish: Local and regional influences on winterkill of fathead minnows in boreal lakes. Trans Am Fish Soc. 2003; 132(2): 289–298.
21. Tonn WM, Magnuson JJ. Patterns in the species composition and richness of fish assemblages in northern Wisconsin lakes. Ecology. 1982; 63(4): 1149–1166.
22. Paine RT. Trophic relationships of 8 sympatric predatory gastropods. Ecology. 1963; 44(1): 63–73.
23. Ozersky T, Bramburger AJ, Elgin AK, Vanderploeg HA, Wang J, Austin JA, et al. The changing face of winter: Lessons and questions from the Laurentian Great Lakes. J Geophys Res Biogeosci. 2021; 126 (6): 25. Available from: https://agupubs.onlinelibrary.wiley.com/doi/full/10.1029/2021JG006247

24. Studd EK, Bates AE, Bramburger AJ, Fernandes T, Hayden B, Henry HAL, et al. Nine maxims for the ecology of cold-climate winters. BioScience. 2021; 71(8): 820–830.

25. Stefan HG, Fang X. Projected climate change effects on winterkill in shallow lakes in the northern United States. Environ Manage. 2000; 25(3): 291–304. https://doi.org/10.1007/s002679910023 PMID: 10629311

26. Rabalais NN, Smith LE, Harper DE, Justic D. Effects of seasonal hypoxia on continental shelf bethos. In: Rabalais NN, Turner RE, editors. Coastal hypoxia: consequences for living resources and ecosystems. Washington, DC.: American Geophysical Union; 2001. pp. 211–240.

27. Salk K, Ostrom PH, Biddanda BA, Weinke AD, Kendal ST, Ostrom NE. Ecosystem metabolism and greenhouse gas production in a mesotrophic northern temperate lake exeriencing seasonal hypoxia. Biogeochemistry. 2016; 131: 303–319.

28. Saarela T, Rissanen AJ, Ojala A, Pumpanen J, Aalto SL, Tiirola M, et al. CH4 oxidation in a boreal lake during the development of hypolimnetic hypoxia. Aquat Sci. 2020; 82(19): 12. Available from: https://link.springer.com/article/10.1007/s00027-019-0690-8

29. Palmer MJ, Chételat J, Jamieson HE, Richardson M, Amyot M. Hydrologic control on winter dissolved oxygen mediates arsenic cycling in a small subarctic lake. Limnol Oceanogr. 2021; 66(S1): S30–S46.

30. McCarthy MJ, Gardner WS, Lehmann MF, Guindon A, Bird DF. Benthic nitrogen regeneration, fixation, and denitrification in a temperate, eutrophic lake: Effects on the nitrogen budget and cyanobacteria blooms. Limnol Oceanogr. 2016; 61(4): 1406–1423.

31. Weinke AD, Bidanda BA. From bacteria to fish: ecological consequences of seasonal hypoxia in a Great Lakes estuary. Ecosystems. 2018; 21: 426–442.

32. Barica B, Gibson J, Howard W. Feasibility of snow clearing to improve dissolved oxygen conditions in a winterkill lake. Can J Fish Aquat Sci. 1983; 40(9): 1526–1531.

33. Fast AW. Winterkill prevention in lakes and ponds using artificial aeration. Reviews in Fisheries Science. 1994; 2(1): 23–77.

34. Schwalme K. A review of winterkill remedation techniques for Alberta. Vegreville: Alberta Environmental Centre; 1995.

35. Pederson DW. Aeration and mixing systems in Minnesota Lakes. St. Paul (MN): Department of Natural Resources, Division of Fish and Wildlife; 1982. Report No. 133.

36. Miller TG, Mackay WC, Walty TD. Under ice water movements induced by mechanical surface aeration and air injection. Lake Reserv Manag. 2001; 17(4): 263–287.

37. Miller TG, Mackay WC. Optimizing artificial aeration for lake winterkill prevention. Lake Reserv Manag. 2003; 19(4): 355–363.

38. McCord SA, Schladow SG, Miller TG. Modeling artificial aeration kinetics in ice-covered lakes. J Environ Eng. 2000; 126(1): 21–31.

39. McCord SA, Schladow SG. Design parameters for artificial aeration of ice-covered lakes. Lake Reserv Manag. 2001; 17(2): 121–126.

40. Ashley KI. Artificial circulation in British Columbia: Review and evaluation. No. 78. Vancouver: Fisheries Technical Circular; 1987.

41. Ellis C, Stefan H. Field testing of an ice-preserving winter lake aeration system. Journal of the American Water Resources Association. 1991; 27(6): p. 903–914.

42. Ashley K, Nordin R. Lake aeration in British Columbia: Applications and experiences. In Murphy T, Munawar M. Aquatic restoration in Canada. Leiden, The Netherlands: Backhuys Publishers; 1999. p. 87–108.

43. Ashley KI. Hypolimnetic aeration: Practical design and application. Water Research. 1985; 19(6): p. 735–740.

44. Schierholz PM, Somervell WL, Babcock W, Hartel R, Timbre K. Wind-powered aeration for remote locations. Springfield, VA:; 1975.

45. Ward PRB, Dunford WG, Ashley KI. Ice control in lakes by photovoltaics powered water circulation. In; 1986; Winnipeg, Manitoba: Proceedings of the Renewable Energy Conferene.

46. Kirke BK. Circulation of reservoirs: A niche market for solar and wind? Renewable Energy Transforming Business. 2000.

47. Ward PB, Cheug EA, Dunford WG, Ashley KI. A directly driven photovoltaic powered pump for water aeration. In; 1989; Penticton, British Columbia: 15th Annual Conference of the Solar Engergy Society of Cananda.

48. Davis MN, McMahon TE, Webb MAH, Ilgen JE, Hitch AT, Jaeger ME, et al. Winter survival, habitat use, and hypoxia tolerance of Montana Arctic Grayling in a winterkill-prone lake. Transactions of the American Fisheries Society. 2019; 148: p. 843–856.

49. Mumma SA, Whitlock C, Pierce K. A 28,000 year history of vegetation and climate from Lower Red Rock Lake, Centennial Valley, Southwestern Montana, USA. Palaeography, Paleaoclimatology, Palaeoecology. 2012; 326-328(30–41): p. 30–41.

50. Gangloff MW. Winter habitat and distribution of Arctic Grayling in upper Red Rock Lake, Red Rock Lakes National Wildlife Refuge, Montana. Bozeman, MT; 1996.

51. U.S. Fish and Wildlife Service. Endangered and threatened wildlife and plants; Revised 12-month finding on a petition to list the upper Missouri River distinct population segment of Arctic Grayling as an endangered or threatened species; 2014.

52. Warren JM, Jaeger M, Gilham A, Cutting K, Bateman L, Paterson T. Centennial Valley Arctic grayling adaptive management project 2018 Spring Update. Various Locations, Montana; 2018.

53. Cutting KA, Cross WF, Anderson ML, Reese EG. Seasonal change in trophic niche of adfluvial Arctic Grayling (Thymallus arcticus) and coexisting fishes in a high-elevation lake system. PLoS ONE. 2016; 11(5): p. e0156187. https://doi.org/10.1371/journal.pone.0156187 PMID: 27205901

54. Cutting KA Ferguson JM, Anderson ML, Cook K, Davis SC, Levine R. Linking beaver dam affected flow dynamics to upstream passage of Arctic grayling. Ecology and Evolution. 2018; 8(24). https://doi.org/10.1002/ece3.4728 PMID: 30619592

55. Montana Fish Wildlife and Parks. Bathymetric GPS survey; 2012.

56. Paullin DG. The ecology of submerged aquatic macrophytes of Red Rock Lakes National Wildlife Refuge Montana. Missoula, MT; 1973.

57. Flynn KF, Johnson TJ, Parker WS, Lovell J. Upper Red Rock Lake, MT: Preliminary engineering and feasibility analysis to improve winter habitat for Arctic Grayling. Helena, MT; 2019.

58. Medora Corporation. SolarBee® SB10000LH Owner's Manual. Dickinson, ND; 2017.

59. EPA. Auxiliary and supplemental power fact sheet: solar power.EPA 832-F-05-011, revised 2007. Washington, DC; 2005.

60. EPA. Auxiliary and Supplemental Power Fact Sheet: Viable Sources. EPA 832-F-05-009. Washington, DC; 2006.

61. Precision Measurement Engineering, Inc. MiniDOT User's Manual. Vista, CA; 2012.

62. MesoWest. [Online].; 2020 [cited 2020 08 06. HYPERLINK "https://mesowest.utah.edu/".

63. R Core Team. R: A language and enviroment for statistical coputing. Vienna, Austria:; 2019.

64. Winslow L, Read R, Woolway J, Brentrup T, Leach T, Zwart J, et al. rLakeAnalyzer: Lake physics tools. R package version 1.11.4.1. [Online].; 2018. HYPERLINK "https://CRAN.R-project.org/package=rLakeAnalyzer".

65. Pebesma E. gstat: Spatial and Spatio-Temporal Geostatistical Modelling, Prediction and Simulation. [Online].; 2020. HYPERLINK "https://CRAN.R-project.org/package=gstat".

66. Schmidt SR, Lischeid G, Hintze T, Adrian R. Disentangling limnological processes in the time-frequency domain. Limnology and Oceanography. 2019; 64(2019): p. 423–440.

67. Bruesewitz DA, Carey CC, Richardson DC, Weathers KC. Under-ice thermal stratification dynamics of a large, deep lake revealed by high-frequency data. Limnology and Oceanography. 2015; 60: p. 347–359.

68. Michel B. Winter regime of rivers and lakes. Cold Regions Science and Engineering Monograph III-B1a. Hanover, NH; 1971.

69. Magnuson JJ, Beckel AL, Mills K, Brandt SB. Surviving winter hypoxia: behavior adaptations of fishes in a northern Wisconsin winterkill lake. Environmental Biology of Fishes. 1985; 14: p. 241–250.

70. Ingole AS, Rakhonde BS. Hybrid power generation system using wind energy and solar energy. International Journal of Scientific and Research Publications. 2015; 5(3): p. 700–703.

71. Hodgkins GAJIC, Huntington TG. Historical changes in lake ice-out dates as indicators of climae change in New England, 1850–2000. International Journal of Climatology. 2002; 22(2002): p. 1819–1827.

72. Arp CD, Jones BM, Whitman M, Larsen A, Urban FE. Lake temperature and ice cover regimes in the Alaskan subarctic and arctic: Integrated montioring, remote sensing, and modeling. Journal of the American Water Resources Assocation. 2010; 46(4): p. 777–791.

73. Bilotta GS, Brazier RE. Understanding the influence of supsended solids on water quality and aquatic biota. Water Research. 2008; 42(2008): p. 2849–2861. https://doi.org/10.1016/j.watres.2008.03.018 PMID: 18462772

74. Bengtsson L. Dispersion in ice-covered lakes. Nordic Hydrology. 1986; 17: p. 151–170.

75. Yang B Wells MG, Li J, Young J. Mixing, stratification, and plankton under lake-ice during winter in a large lake: Implications for spring dissolved oxygen levels. Limnology and Oceanography. 2020 July; 6.

76. Rogers CK, Lawrence GL, Hamblin PF. Thermal impact of artificial circulation on an ice-covered mid-latitude lake. Canadian journal of civil engineering. 1996; 23(5): p. 1081–1091.